

# THE NUCLEAR PERMEABILITY, INTRACELLULAR DISTRIBUTION, AND DIFFUSION OF INULIN IN THE AMPHIBIAN OOCYTE

SAMUEL B. HOROWITZ and LEONARD C. MOORE

From the Laboratory of Cell Physiology, Department of Biology, Michigan Cancer Foundation,  
Detroit, Michigan 48201

## ABSTRACT

[<sup>3</sup>H]Inulin (mol wt  $\approx$  5,500) solutions are microinjected into the cytoplasm of mature oocytes of *Rana pipiens* and the subsequent movement of the solute recorded by quantitative ultralow temperature autoradiography. The autoradiographs show transient cellular diffusion gradients, the influence of the nucleus on these gradients, and the nuclear:cytoplasmic distribution of inulin. Analysis leads to the following conclusions: (a) Inulin diffuses in cytoplasm at about  $3 \times 10^{-6}$  cm<sup>2</sup>/s, or one-fifth as rapidly as in water. Most of this decrease is attributable to the increased tortuosity of the diffusional path due to the presence of inclusions and macromolecules. (b) The nuclear envelope is very permeable to inulin; its resistance to inulin's passage is similar to that of cytoplasm. The envelope appears to play a negligible role in regulating the nucleocytoplasmic movement of solutes smaller than macromolecules. (c) Inulin concentrates in the nucleus to four times its cytoplasmic level; this is attributed to solute exclusion from cytoplasmic water. Evidence is presented that among hydrophilic solutes the degree of exclusion increases with molecular size. The potential significance of cytoplasmic exclusion processes to understanding secretion and the intracellular movement of macromolecules is briefly discussed.

## INTRODUCTION

The location and properties of the intracellular barriers to solute movement is one of the least explored areas of cell biology. There are technical reasons for this: the plasma membrane masks many of the transport events occurring within its confines; the properties of intracellular transport barriers change during experimental manipulation; and it is difficult to localize and measure solutes in the small intracellular space. Nature has not been generous in providing cellular systems in which it has proved possible to overcome these difficulties. An exception is the mature amphibian oocyte which provides an exceptionally good

material for study because of its large size, the large size of its nucleus, and its "normal" transport properties (14).

This paper is one of a number in which we analyze the distribution and movement of solutes in the oocyte, particularly the more general transport characteristics of the intracellular space: the diffusional properties of cytoplasm, the permeability properties of intracellular membranes, and the factors determining the distribution of solutes between nucleus and cytoplasm. We anticipate this analysis will have direct relevance to a number of important but poorly understood

cellular processes, including the nucleocytoplasmic commerce in information-bearing macromolecules, the control of metabolite movements from sources to sinks, and the process of secretion.

In the present experiments a solution of the polysaccharide [ $^3\text{H}$ ]inulin, mol wt about 5,500 (24, 34), is injected into the cytoplasm of *Rana pipiens* oocytes and intracellular inulin gradients allowed to develop. Diffusion is terminated by quenching the oocytes in liquid nitrogen at  $-190^\circ\text{C}$ . They are sectioned at  $-50^\circ\text{C}$  and their local cytoplasmic and nuclear inulin concentrations determined by ultralow temperature autoradiography (13).

The greatest inulin concentration occurs at the injection site and decreases progressively with distance from this point. After injection the solute concentration gradient briefly conforms to theoretical diffusion gradients and can be used to determine diffusion coefficients in cytoplasm. In time, the gradient reaches the cell membrane, where it is distorted from its simple diffusional character. The spreading gradient finally becomes transcellular, invests the nucleus, and ultimately reaches diffusional equilibrium.

When the nucleus sits astride the diffusional gradient one can discern its influences on the gradient and can deduce the permeability of the nuclear envelope, the nucleocytoplasmic distribution of the solute, and something of nucleoplasm's diffusional properties.

In an earlier microinjection study (12) the solute was the disaccharide sucrose (mol wt = 342). (That paper provides a full description of the design and rationale of these experiments.) Inulin has chemical properties similar to sucrose, but its size places it at the low end of the macromolecular range. We therefore expect comparison of the sucrose and inulin results to provide information on the way variation in molecular size influences the intracellular transport processes under investigation.

## MATERIALS AND METHODS

### Oocytes

*Rana pipiens*, obtained in November and December, were kept in spring water at  $4^\circ\text{C}$  until use.

The oocytes were mature, stage  $\text{Y}_5$  of Kemp (17). Their isolation from the ovary into Ringer's solution and the physical characteristics of the cells are described elsewhere (1, 14).

### Solutions

The Ringer's solution was described previously (12).

[ $^3\text{H}$ ]Inulin was obtained as crystals from Schwarz/Mann, Div. Becton, Dickinson & Co., Orangeburg, N. Y., Lot no. 7001 P, sp act 450 mCi/g.

Purification removed low molecular weight material from the [ $^3\text{H}$ ]inulin to be injected, and was accomplished with two passes through a  $60 \times 0.9$  cm column of Sephadex G-25. The dashed line in Fig. 1 represents the chromatograph of the first pass. The area of single hatching is the volume of the first pass used for the second pass; it coincides with the void volume measured with blue dextran 2000. Before being rerun, this fraction was lyophilized and resuspended in 0.3 ml of water. The solid line in Fig. 1 represents the chromatograph of the second pass. The volume of effluent indicated by cross-hatching was lyophilized and used as the injectate after resuspension in water. The injectate contained 8.6 mg/ml of inulin with an activity of 3.9 mCi/ml.

### Microinjection

Microinjection was made into the vegetal hemisphere to avoid damaging the nucleus. Injected volumes were 0.6 to  $3.9 \times 10^{-6}$  cm $^3$ , or 0.02 – 0.16% of oocyte volumes. The procedure was described previously (12).

After injection, oocytes were transferred to a chamber where they sat in a drop of Ringer's solution on a pad of filter paper. The time ( $t$ ) between microinjection and quenching in liquid nitrogen is the period when solute diffusion occurs. The times sampled are from 479 to 20,000 s ( $\approx$  0.13–5.6 h).

### Autoradiography

The autoradiographic technique is detailed elsewhere (13–15). It involves (a) freezing the oocyte to liquid nitrogen temperatures in a medium that permits low temperature sectioning; (b) sectioning at  $-50^\circ\text{C}$ , after which the sections are brought into contact with dry, cold photographic emulsion; (c) exposure at  $-85^\circ\text{C}$ ; and (d) development, bleaching, and mounting of autoradiographs.

Exposure times,  $t_e$ , varied from 5.8 to 112 days to achieve optimum grain densities for quantitative analyses. Shorter exposure times tend to coincide with shorter diffusion times when the injectate has not been diluted by diffusion in the oocyte.

### Grain Counting and Quantification

Grain densities were determined at magnifications of 2,000 or 2,500, in phase-contrast illumination, using a Whipple-Hauser type eyepiece micrometer.

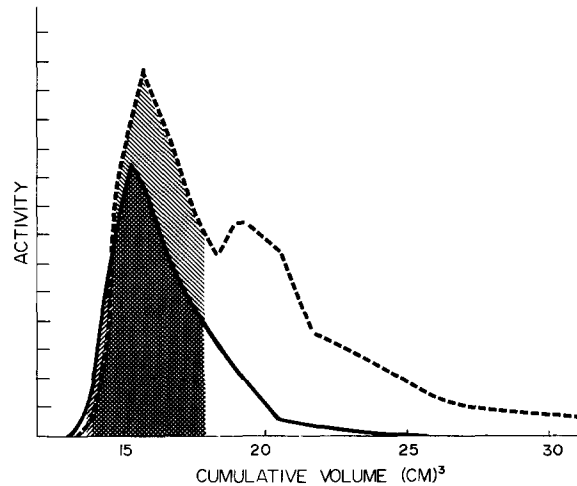


FIGURE 1 Purification of  $[^3\text{H}]$ inulin for microinjection by two successive passes through a column of Sephadex G-25. See text for explanation.

Background and nonlinearity corrections, described in detail elsewhere (13, 14), were made to ensure that grain density is proportional to the tritium content of the section. Grain densities,  $G$ , are expressed as grains per  $1,000 \mu\text{m}^2$  per hour of autoradiographic exposure.

Autoradiographic spatial resolution is at least  $3 \mu\text{m}$ , the value previously reported for  $[^3\text{H}]$ sucrose (12).

## RESULTS

### *Injection Site and Cytoplasmic Diffusion Gradients*

Fig. 2 shows a grain density profile through an injection site at  $t = 479$  s. There are two components to the profile. A sharp peak at the injection site, indicated by a broken line, is superimposed on a less steep cytoplasmic gradient. The peak marks the injectate itself, which has not completely dispersed. A regular feature in these experiments, it is seen as long as 20,000 s after microinjection. The cytoplasmic gradient is due to the diffusion of  $[^3\text{H}]$ inulin away from the injection site. Its form agrees well with a theoretical diffusion profile shown as a solid line.

The experimental data presented in Fig. 2 are derived from two transects taken at right angles to each other through the injection site. Their paths are shown in the inset: the solid circles are from A to B, the open circles from C to D. The similarity in the grain density-distance relation-

ship of these transects clearly indicates that insulin diffusion is isotropic in cytoplasm.

The cytoplasmic diffusion coefficient for inulin can be estimated by comparing the observed cytoplasmic gradient to theoretical diffusion profiles. Assuming that the injection volume is sufficiently small to constitute an instantaneous point source and that solute reflection from the cell boundary is negligible, then

$$G_r = \left[ \frac{A}{8(\pi D_c t)^{3/2}} \right] e^{-r^2/4D_c t} \quad (1)$$

describes the grain density ( $G_r$ ) due to  $[^3\text{H}]$ inulin at locations along radii emanating from the injection site (5).  $D_c$  is inulin's diffusion coefficient,  $r$  the radial distance from the injection site, and  $A$  a scaling constant defined so that  $G_r$  at  $r = 0$  is that actually observed.

Comparison of theoretical profiles and experimentally determined points is made by setting the bracketed term in Eq. 1 equal to the observed grain density at the highest point on the cytoplasmic gradient,  $0.147$  grains/ $1,000 \mu\text{m}^2$  per h, and substituting various values of  $D_c$ . The solid line in Fig. 2 is for  $D_c = 4.0 \times 10^{-7}$   $\text{cm}^2/\text{s}$  and provides a good fit of the profile. Deviation from theory is appreciable only where the diffusing inulin approaches the cell surface on the left. We attribute this deviation to reflection from the plasma membrane.

A peculiarity of the profiles in Fig. 2 is the acentric peak in both gradients, displaced about 100

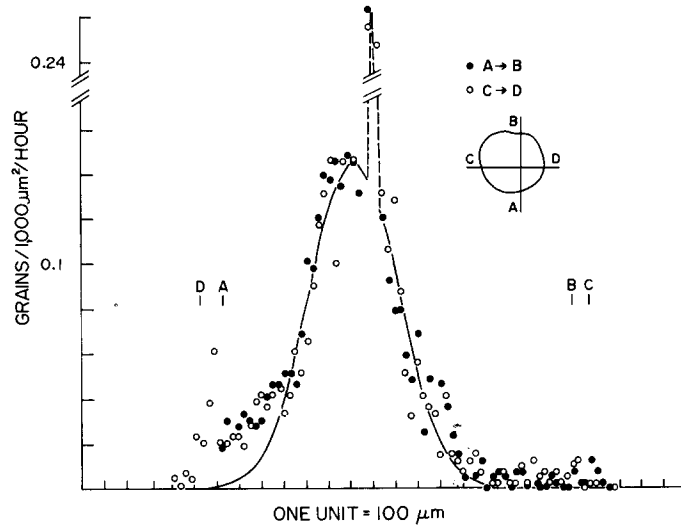


FIGURE 2 Two grain density profiles taken perpendicular to each other through the injection site and cytoplasm of an oocyte injected with  $[^3\text{H}]\text{inulin}$ .  $t = 479$  s. The vertical bars (A-D) mark the cell boundaries as indicated in the *inset*. Points are experimental; solid line is theoretical. See text for additional explanation.

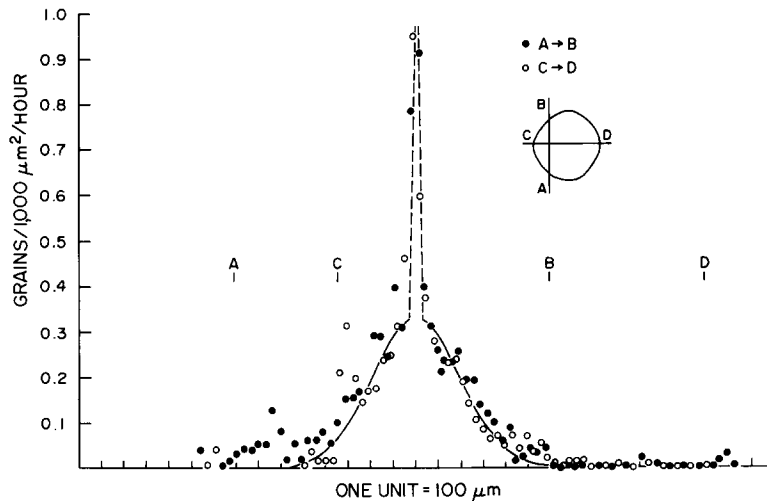


FIGURE 3 Two grain density profiles taken perpendicular to each other through the injection site and cytoplasm of an oocyte injected with  $[^3\text{H}]\text{inulin}$ .  $t = 966$  s. The vertical bars (A-D) mark the cell boundaries as indicated in the *inset*. The injection site is at the juncture of the transects A  $\rightarrow$  B and C  $\rightarrow$  D. Points are experimental, solid line is theoretical. See text for additional explanation.

$\mu\text{m}$  from the center of the cytoplasmic gradient, upward and to the left of the junction of lines A-B and C-D. This is the only such acentricity encountered in either the sucrose or inulin studies. An elongated or crescent-shaped injection site might account for the occurrence, but detailed examination of the sections provides no positive explanation.

Fig. 3 shows two grain density profiles through the injection site of an oocyte at  $t = 966$  s. These profiles are perpendicular to each other, as indicated in the inset, and are qualitatively similar to those in Fig. 2. Diffusion is isotropic. A sharp peak marks the injection site, which here is concentric with the diffusion gradient. The experimental points conform well to a theoretical diffusion

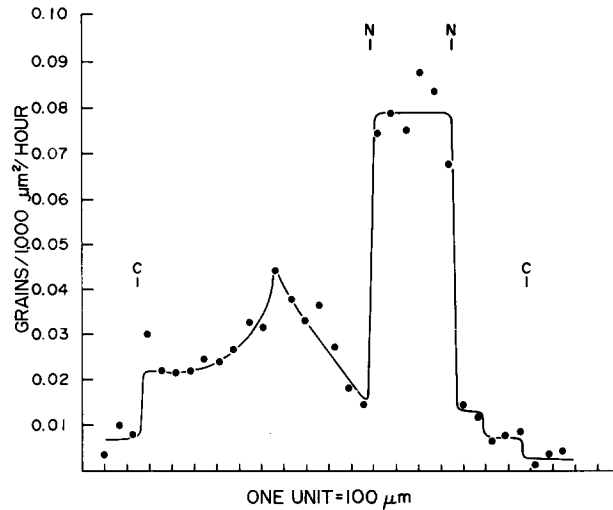


FIGURE 4 Grain density profile through the cytoplasm and nucleus of an oocyte injected with  $[^3\text{H}]$ inulin.  $t = 3,127$  s. The vertical bars mark the cell (C) and nuclear (N) boundaries. Points experimental, line fitted. See text for additional explanation.

profile (solid line) derived from Eq. 1. As in Fig. 2, deviation from the theoretical diffusion profile occurs only where the gradient approaches the cell membrane segment closest to the injection site: the cell border shown as the arc B-C-A.

The theoretical line in Fig. 3 was obtained by setting the bracketed term in Eq. 1 equal to 0.335 grains/1,000  $\mu\text{m}^2$  per h and  $D_e = 2 \times 10^{-7}$   $\text{cm}^2/\text{s}$ . Taken with the value for  $D_e$  derived from the  $t = 479$  s experiment, an average value for  $D_e = 3 \times 10^{-7}$   $\text{cm}^2/\text{s}$  results.

In the oocytes of the next longest time group ( $\approx 3,000$  s) the diffusing inulin piled up at the cell membrane sufficiently to greatly complicate the gradients as seen in Fig. 4. Although we have not tried to calculate  $D_e$  from these longer time experiments, it is clear that the gradients here observed are consistent with estimates of  $D_e$  made from shorter time experiments.

### Nucleus

Examination of grain density profiles that pass through both cytoplasm and nucleus establishes several points about nuclear transport. Typical are those shown in Figs. 4-6 for oocytes frozen at approximately 3,000, 6,000, and 20,000 s after microinjection. All have similar characteristics: (a) A cytoplasmic concentration gradient (which becomes less acute with time). (b) The nuclear concentration of  $[^3\text{H}]$ inulin is higher than that of

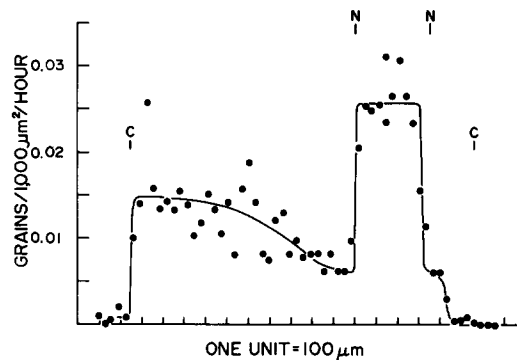


FIGURE 5 Grain density profile through the cytoplasm and nucleus of an oocyte injected with  $[^3\text{H}]$ inulin.  $t = 5,993$  s. The vertical bars mark the cell (C) and nuclear (N) boundaries. Points experimental, line fitted. See text for additional explanation.

the adjacent cytoplasm, and the rise occurs as a step function at the nuclear boundary. (c) The concentration of  $[^3\text{H}]$ inulin is uniform across the entire nucleus.

The increase in grain density over the nucleus is due in part to the high water content of the nucleus. The cytoplasm of the mature oocyte, because it contains yolk and other dense inclusions, is about 45% water, while the nucleus is about 85% water (4). In other words, 1.9 times as much water is present in a volume of nucleus as in an equal volume of cytoplasm. Since grain density is proportional to radioactivity on a volume basis,

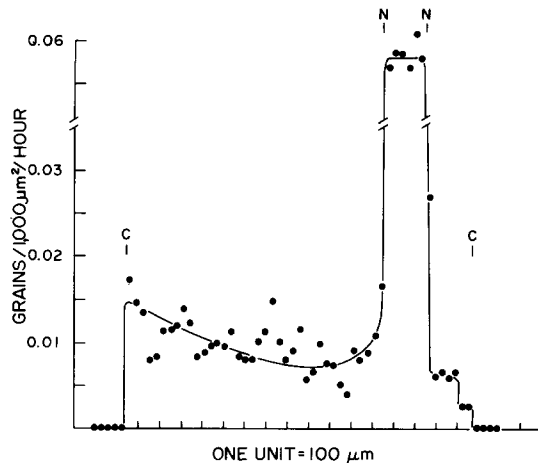


FIGURE 6 Grain density profile through the cytoplasm and nucleus of an oocyte injected with  $[^3\text{H}]\text{inulin}$ .  $t = 20,000$  s. The vertical bars mark the cell (C) and nuclear (N) boundaries. Points experimental, line fitted. See text for additional explanation.

when the grain density profile of a water-soluble material passes from cytoplasm to nucleus, it exhibits a 1.9 increase even when no difference in solute concentration exists.

It is important to note that the difference in cytoplasmic and nuclear inulin concentrations is much greater than can be accounted for by the difference in water content alone. To compare nuclear and cytoplasmic contents we determine grain density,  $G$ , at positions ( $a, b, c, \dots$ ) inside but along the edge of the nucleus ( $G_n^a, G_n^b, \dots$ ) and in the immediately adjacent cytoplasm ( $G_c^a, G_c^b, \dots$ ). This normalizes the data for cytoplasmic gradients. The mean of the ratios of adjacent nuclear and cytoplasmic sites

$$\bar{X}_{n/c} = [G_n^a/G_c^a + G_n^b/G_c^b + \dots]/N \quad (2)$$

is very close to the true ratios of the inulin concentrations on a volume basis.<sup>1</sup>

Table I gives  $\bar{X}_{n/c}$  for those oocytes whose nuclear and cytoplasmic raw grain densities permit reliable determinations of  $G_n$  and  $G_c$ . Corrected for the difference in water content of cytoplasm and nucleus, the ratios  $K_{n/c}$  are from 3.1 to 4.4 with a mean of  $4.0 \pm 0.5$ . These vary independently of  $t$ , which implies that once inulin reaches the perimeter of the nucleus, it experiences

<sup>1</sup> Small differences in autoradiographic efficiency arise from the differing compositions of nucleus and cytoplasm. These are discussed in reference 14.

TABLE I  
The Ratios of the Concentrations of  $[^3\text{H}]\text{inulin}$  in Nucleus and Cytoplasm

Time after injection (s)	Nuclear : cytoplasmic grain density ratio ( $X_{n/c} \pm \text{SE}$ )	Concentration ratio on water basis ( $K_{n/c}$ )
3,011	$7.42 \pm 0.40$	3.9
3,127	$8.17 \pm 0.41$	4.3
5,993	$5.93 \pm 0.20$	3.1
6,005	$8.26 \pm 0.55$	4.3
20,000	$8.30 \pm 0.33$	4.4
	Mean = $7.45 \pm 0.17$	$4.0 \pm 0.5$

no significant delay in crossing the nuclear envelope.

None of the nuclear profiles show evidence of an inulin concentration gradient parallel to that in the cytoplasm—a surprising observation, since nuclear gradients were a regular feature in the sucrose study (12). The absence of nuclear gradients, along with evidence for the lack of a transport barrier at the nuclear surface, implies that diffusion of insulin is appreciably more rapid in nucleoplasm than in cytoplasm.

## DISCUSSION

### Nuclear Transport

The constancy of  $\bar{X}_{n/c}$  with time, shown in Table I, indicates that after reaching the perinuclear region inulin experiences little additional delay before it enters the nucleus. In this respect inulin transport is similar to that of sucrose (12). The nuclear membrane appears to present no more of a barrier to the diffusion of these solutes than a comparable structure composed of cytoplasm.

The sucrose and inulin results differ regarding the solute distribution observed in nuclei invested in a cytoplasmic solute gradient. In sucrose, cytoplasmic gradients have corresponding nuclear gradients of similar slope and direction. We infer from this that the nuclear envelope not only is not an effective barrier, but the diffusional resistance offered by the nucleoplasm is roughly equal to that offered by cytoplasm. The distribution of inulin in nuclei invested in a cytoplasmic gradient *does not* reflect the cytoplasmic gradient but shows a uniform distribution. Since membrane resistance is negligible, this indicates that inulin's diffusion in nucleoplasm is more rapid than its diffusion in cytoplasm. It follows that the ratio of nuclear to

cytoplasmic diffusion coefficients must be greater for inulin than for sucrose.

The ease with which inulin passes the nuclear envelope was not unexpected. Gurdon (10) demonstrated that much larger molecules, the histones (mol wt = 10,000–20,000) and bovine serum albumin (mol wt = 67,000), enter the *Xenopus* oocyte nucleus after cytoplasmic microinjection. More recently, Paine and Feldherr (23), working with the cockroach oocyte, used a series of fluorescein-labeled proteins of mol wt 12,398–67,000. They found no sharp cutoff point but a steep decrease in permeability between proteins of mol wt 17,816 and 44,300 (myoglobin and ovalbumin, respectively). Furthermore, our work in progress with size-graded dextrans indicates an effective pore size in the amphibian oocyte consistent with the cockroach results.

### Nucleocytoplasmic Distribution and Cytoplasmic Solute Exclusion

The ratio of nuclear to cytoplasmic inulin concentrations on a water basis,  $K_{n/c}$ , is 4.0 (Table 1). The ease with which inulin passes the nuclear envelope disqualifies active transport as an explanation for this marked accumulation. Two possibilities are more likely: (a) Inulin is adsorbed on nuclear macromolecular components so that nuclear concentrations exceed those of cytoplasm, i.e., binding. (b) Inulin is excluded from much of the water of cytoplasm but to a lesser degree from nuclear water. The choice between these alternatives is abetted by considering glycerol and sucrose, other polyols for which data are available.

When intact oocytes are bathed in glycerol-Ringer solution of concentration  $g$ , the nuclear concentration of freely diffusing glycerol at equilibrium is 0.96 g, while the cytoplasmic concentration is 0.73 g. The ratio  $K_{n/c}$  is therefore 1.3 (14). The simplest explanation for these observations is that cytoplasm differs from both the bathing solution and nucleus in partially excluding glycerol. One need not invoke nuclear binding to explain the observed  $K_{n/c}$ . Ideally, we would do a parallel distribution study with sucrose and inulin, but the inability of these solutes to permeate the oocyte plasma membrane prevents this. However, other evidence also supports the water exclusion model for these solutes.

First, in exclusion systems solute concentration occurs in the solvent-rich phase at the expense of the solvent-deficient macromolecular matrix (the

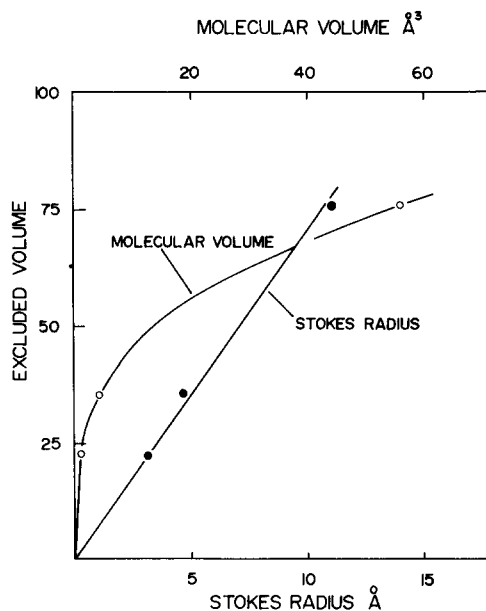


FIGURE 7 Cytoplasmic excluded volume as a function of molecular volume (open circles) from Eq. 4, and Stokes radius (closed circles) from Eq. 3 for three polyols. Excluded volume for glycerol from reference 14 and sucrose from reference 12.

converse is expected in binding systems). Examples of excluding systems are cross-linked dextran and polyacrylamide gels used in chromatography. The oocyte resembles these in concentrating glycerol, sucrose, and inulin in its water-rich nucleus.

Second, exclusion processes typically show molecular specificity in which the asymmetry between solvent-rich and polymer-rich phases increases with solute size (2, 6). The oocyte shares this specificity as seen in the increase of  $K_{n/c}$ , demonstrated graphically in Fig. 7 and discussed below. In this regard, saccharides, without ionizable groups or hydrophobic segments, probably lack a physical basis for generalized size-related binding.<sup>2</sup>

Third,  $K_{n/c}$  values greater than unity are mirrored in the distribution of solutes between the injection water and adjacent cytoplasm. This is seen in Figs. 2 and 3, where a pool of inulin persists at the injection site though surrounded by

<sup>2</sup> We do not ignore the possibility of stereospecific H bonding which may be involved in the membrane transport of glycerol and sucrose in certain cells (8, 29), but we do not expect this to correlate with size.

cytoplasm at a much lower concentration. Sucrose behaves in a similar manner (12). Since the injectate does not contain binding material, the probable explanation for the low absorption of both inulin and sucrose (and their osmotically held water) is low solubility in the water of cytoplasm, that is, solute exclusion.

We conclude that cytoplasmic solute exclusion is the most likely explanation for the nuclear accumulation of the solutes studied. As mentioned, about 96% of the nuclear water is available as solvent for glycerol (14). If the same holds true for inulin, then the  $K_{n/c}$  of 4.0 implies that 76% of the cytoplasmic water is unavailable as solvent.<sup>3</sup>

Fig. 7 is a plot of cytoplasmic excluded volume derived from  $K_{n/c}$  for three solutes as a function of two measures of molecular size, the equivalent Stokes radius,  $r$ , from

$$r = \left( \frac{3Mv}{4\pi N} \right)^{1/3} \quad (3)$$

and molecular volume,  $V$ , from

$$V = \frac{Mv}{N} \quad (4)$$

in which  $M$  is molecular weight,  $v$  is the partial specific volume in aqueous solution, and  $N$  is Avogadro's number.

Fig. 7 derives from limited data but suggests that a relationship exists between the cytoplasmic water volume denied to a solute and the solute's Stokes radius. If additional evidence supports this relationship, it may help understand a number of cellular processes and the organization of the cell's interior.

For example, the cytoplasmic exclusion of macromolecules, if tied to the synthetic activity of the cell, provides a simple model for some secretory processes. One can visualize a process involving the entry of monomeric substances into a cell, their synthesis into macromolecules, and the latter's concentration and subsequent expulsion from the cell due to excluded volume processes. We suggested earlier (12) that these processes may be important in concentrating and packaging the products of synthesis for export from the cell.

The exclusion model for secretion assumes that

<sup>3</sup> This figure is even greater if the nucleus itself excludes inulin relative to aqueous solution to a greater extent than it excludes glycerol.

such cytoplasmic organelles as the cisternae of the endoplasmic reticulum (ER) and the Golgi apparatus have solubility properties more akin to free solution than those of the remaining cytoplasm, and that exclusion leads to solute concentration in these compartments. It draws attention to the solvent properties of the cisternal and vesicular contents of organelles, rather than the permeability of their membranes, as important in understanding secretion.

The proposed model implies that proteins of ground cytoplasm "recognize" each other to the partial or total exclusion of other macromolecules. A number of mechanisms can be involved in this, the simplest being that the proteins of cytoplasm are organized by intermolecular forces into discrete domains which are the excluding units. The interstices between these domains, then, are the location of the soluble macromolecules in cytoplasm.<sup>4</sup> In this view the ER and Golgi cisternae are considered specialized membrane-bordered interstitial spaces.

The nucleus also can be viewed as a specialized interstice where transcription and replication occur in a milieu uncluttered by the macromolecules and inclusions responsible for the cell's "physiological" activities. If this notion is correct, then nonstructural proteins smaller than those restricted by the nuclear membrane can be expected to move between nucleus and cytoplasmic interstices while being excluded from the cytoplasmic domains. A series of experiments by Goldstein, Prescott, and their associates can be interpreted in this light.

These workers demonstrated that when a [<sup>3</sup>H]-amino acid-labeled nucleus of *Amoeba proteus* is transplanted into another individual, about 40% of the labeled nuclear material rapidly redistributes. This material, called RMP, appears to be a heterogeneous population of water-soluble proteins. In the new distribution RMP concentrates in the nuclei of the binucleate cell equally, but is only 2-4% as concentrated in the cytoplasm as in the nuclei (9, 16). At mitosis nuclear RMP disperses into the cytoplasm and reconcentrates when the nucleus reforms (26). We suggest the be-

<sup>4</sup> In general, the larger a soluble molecule, the more it will concentrate in the interstices of an excluding system. This relation may explain why secretory proteins, in the period between synthesis and emiocytosis, are linked to large functionally inert peptide chains (30).



havior of RMP can be understood by viewing it as the cell's population of smaller soluble proteins with an average excluded cytoplasmic volume on the order of 96%.

If the explanation for the RMP phenomenon observed in *Amoeba* lies in excluded volume processes, important implications follow: (a) cytoplasmic-excluded volume processes are widespread and important in cells other than the amphibian oocyte, and (b) a substantial part of the soluble macromolecular content of cells is excluded from the cytoplasmic domains and restricted to cytoplasmic interstices and organelles, like the nucleus, with interstice-like solubility properties.

Exclusion processes provide a mechanism for ordering and controlling intracellular solute commerce by restricting the intracellular distribution and movement of solutes to defined regions and paths. There is evidence that specific mechanisms exist to utilize this cytoplasmic property. As an example, the intracellular distribution of steroids in hormone-responsive cells is determined by whether they are bound to specific soluble protein receptors. The nonbinding steroid [<sup>3</sup>H]-norethynodrel distributes between the nucleus and cytoplasm of rat uterus epithelium in the ratio of 0.2:1, while [<sup>3</sup>H]estradiol, which binds, distributes in the ratio of 4.6:1, an enhancement of nuclear concentration by a factor of 23 (31). An interesting detail of this process is that receptor protein (mol wt  $\approx$  118,000) splits before entering the nucleus, its penetration of the nuclear membrane possibly requiring a reduction in mol wt to about 60,000 (27, for review see reference 32).

### Diffusion in Cytoplasm

The diffusion coefficient of inulin in the oocyte's intact cytoplasm,  $D_c$ , is  $3 \times 10^{-7}$  cm<sup>2</sup>/s; in water it is  $1.48 \times 10^{-6}$  cm<sup>2</sup>/s.<sup>5</sup> The ratio of the two,

<sup>5</sup> Two methods have been used to determine inulin's diffusion coefficient in water. In one, diffusion is between two compartments of pure water (3, 22) and in a second, diffusion is from water into a dilute agar gel (18, 25, 33).  $D_w$  obtained by the former method averages  $1.48 \times 10^{-6}$  cm<sup>2</sup>/s (range 1.33 to  $1.6 \times 10^{-6}$  cm<sup>2</sup>/s); by the latter method,  $1.87 \times 10^{-6}$  cm<sup>2</sup>/s (range 1.62 to  $2.08 \times 10^{-6}$  cm<sup>2</sup>/s). (All values are corrected to 20°C by the equation  $D_2 = D_1 T_2 \eta_1 / T_1 \eta_2$ , where  $D$  is the diffusion coefficient,  $T$  the absolute temperature, and  $\eta$  the coefficient of viscosity of water.) The values obtained

$D_c/D_w$ , is 0.20—a relatively large value—which suggests that the transport properties of cytoplasm are only slightly different from water's. The simplest explanation credits the ratio to the increased tortuosity of diffusion caused by cytoplasm's high concentrations of yolk platelets, pigment granules, other inclusions, and protein. If this is the case,

$$D_c = D_w/\lambda^2, \quad (5)$$

where  $\lambda$  is the factor by which the diffusional path has increased (21). The value of  $\lambda$  is 2.2, which implies that if only tortuosity is involved, inclusions have effectively doubled the path necessarily traversed by inulin diffusing between points in cytoplasm.

The tortuosity hypothesis appears to explain most studies of cytoplasm's slowing effect on the diffusion of solutes. This can be seen from the application of the Mackie and Meares (21) equation for tortuosity in water-swollen polymer-systems

$$D_c/D_w = \left( \frac{1 - v_r}{1 + v_r} \right)^2 \quad (6)$$

in which  $v_r$  is the volume fraction of the water-polymer system inaccessible to the solute. In the present system

$$v_r = v_p + v_s, \quad (7)$$

where  $v_p$  is the volume fraction of polymer, taken as the volume fraction of oocyte dry weight (0.43), and  $v_s$  the volume fraction of water from

using the gel system are consistently higher than those in water. This is suspect since the effect of agar is likely to slow rather than increase diffusion (7). A systematic error seems to be associated with determinations made in the water-gel system; however, it is not intrinsic to the technique since comparable deviations are not found for other solutes (28). A factor which may account for these errors is that all the agar studies used commercial labeled inulin without additional purification, while the pure water studies were performed with unlabeled inulin. Fig. 1 shows that the commercial [<sup>3</sup>H]inulin used in this study had a large amount of low molecular weight contaminant which had to be removed by chromatography. In our experience such contamination is a regular feature of commercial labeled polysaccharides.

Because the values for  $D_w$  obtained by the isotope-gel system are compromised we used  $D_w = 1.48 \times 10^{-6}$  cm<sup>2</sup>/s in our calculations.

TABLE II  
*The Relative Rates of Diffusion in Cytoplasm and  
 Pure Water Determined Experimentally and  
 Calculated from Eq. 6*

	$D_c/D_w$ (experimental)	$D_c/D_w$ (calculated)	Exp/Cal
Sucrose	0.38	0.50	0.76
Inulin	0.20	0.36	0.56

which solute is excluded. Table II gives the experimentally derived and calculated values for  $D_c/D_w$  for sucrose and inulin.

The tortuosity model accounts for 76% and 56%, respectively, of the slowing of sucrose and inulin diffusion. Since error in estimating  $D_c$  may be as high as 50%, tortuosity alone could explain our results. Other mechanisms that might contribute to diffusional slowing are solute-polymer interactions and diffusion in water modified by hydration.

Hydration probably can be ruled out as significant, since it is a solvent-polymer interaction and, if appreciable, would result in water diffusion being slower than can be explained by tortuosity. This is not the case. We can estimate  $v_r$  for water in the oocyte from published values of the diffusion coefficient. Hansson Mild et al. (11), using nuclear magnetic resonance, found the water diffusion coefficient<sup>6</sup> to be  $0.68 \times 10^{-5}$  cm<sup>2</sup>/s; hence  $D_c D_w$  for water is about 0.33 and from Eq. 6,  $v_r = 0.27$ . This is less than  $v_p$  and implies that the tortuosity provided by the dry material of cytoplasm alone is more than sufficient to account for its diffusion slowing effect on water. Other values of  $D_c$  for water have been reported (19, 20), but these are even higher. It appears that water sorption to macromolecules (hydration) in oocyte cytoplasm is at most marginally significant to diffusion.

Based on these observations, we view oocyte cytoplasm as a heterogeneous medium in which a continuous interstitial phase has the diffusional and solubility properties of ordinary aqueous solution. Distributed in this is a semicontinuous or discontinuous macromolecular matrix which limits, by steric hindrance, the solubility (and presumably the diffusion) of polar molecules as a function of their size. Our evidence disputes the

<sup>6</sup> The nucleus is only 2.4% of the total cell volume and its contribution can be ignored.

notion that water associated with the macromolecular matrix is appreciably modified from the free solution condition.

The nucleoplasm seems to have the solubility properties of the cytoplasmic interstitium, with which it freely exchanges solutes at least as large as inulin. The transport properties of the nuclear membrane are apparently important only in limiting the nucleocytoplasmic movement of particulate matter and macromolecules. Its cutoff point for molecular sieving is under investigation.

The authors wish to thank Doctors Philip Paine, Stanley Rapaport, and Marvin A. Rich for useful suggestions, and Mss. Marian S. H. Horowitz and Jean Reeves for editorial assistance.

This work was supported by National Institute of Health grant GM 19548, National Science Foundation grant GB 27981, and an institutional grant to the Michigan Cancer Foundation from the United Foundation of Greater Detroit.

Received for publication 30 July 1973, and in revised form 15 October 1973.

#### REFERENCES

- ABELSON, P. H., and W. R. DURYEE. 1949. *Biol. Bull. (Woods Hole)*. **96**:205.
- ACKERS, G. K. 1964. *Biochemistry*. **3**:723.
- BUNIM, J. J., W. H. SMITH, and H. W. SMITH. 1937. *J. Biol. Chem.* **118**:667.
- CENTURY, T. J., I. R. FENICHEL, and S. B. HOROWITZ. 1970. *J. Cell Sci.* **7**:5.
- CRANK, J. 1956. *The Mathematics of Diffusion*. The Oxford University Press, London.
- FISCHER, L. 1969. *An Introduction to Gel Chromatography*. North-Holland Publishing Co., Amsterdam.
- FRIEDMAN, L. 1930. *J. Am. Chem. Soc.* **52**:1311.
- FUKUI, J., and R. M. HOCHSTER. 1964. *Can. J. Biochem.* **42**:1023.
- GOLDSTEIN, L., and D. M. PRESCOTT. 1967. *J. Cell Biol.* **33**:637.
- GURDON, J. B. 1970. *Proc. R. Soc. Lond. B. Biol. Sci.* **176**:303.
- HANSSON MILD, K., T. L. JAMES, and K. T. GILLEN. 1972. *J. Cell Physiol.* **30**:155.
- HOROWITZ, S. B. 1972. *J. Cell Biol.* **54**:609.
- HOROWITZ, S. B. 1973. *In Methods in Cell Physiology*. Vol. 8. D. M. Prescott, editor. Academic Press Inc., New York. 249.
- HOROWITZ, S. B., and I. R. FENICHEL. 1968. *J. Gen. Physiol.* **51**:703.
- HOROWITZ, S. B., and I. R. FENICHEL. 1970. *J. Cell Biol.* **47**:120.

16. JELINEK, W., and L. GOLDSTEIN. 1973. *J. Cell Physiol.* **81**:181.
17. KEMP, N. E. 1953. *J. Morphol.* **92**:487.
18. LANMAN, R. C., J. A. BURTON, and L. S. SCHANKER. 1971. *Life Sci.* **10**:803.
19. LING, G. N., M. M. OCHSENFELD, and G. KARREMAN. 1967. *J. Gen. Physiol.* **50**:1807.
20. LØVTRUP, S., K. HANSSON MILD, and A. BERGLUND. 1970. *J. Cell Physiol.* **76**:167.
21. MACKIE, J. S., and P. MEARES. 1955. *Proc. R. Soc. Lond. A.* **232**:496.
22. ÖHOLM, L. W. 1912. *Medd. K. Vetenskapakad. Nobel Inst.* **2**(23):1.
23. PAINE, P. L., and C. M. FELDHERR. 1972. *Exp. Cell Res.* **74**:81.
24. PHELPS, C. F. 1965. *Biochem. J.* **95**:41.
25. POLLAY, M., A. STEVENS, and R. KAPLAN. *Anal. Biochem.* **27**:381.
26. PRESCOTT, D., and L. GOLDSTEIN. 1968. *J. Cell Biol.* **39**:404.
27. PUCA, G. A., E. NOLA, V. SIGA, and F. BRESCIANI. 1972. *Biochemistry.* **11**:4157.
28. SCHANTZ, E. J., and M. A. LAUFFER. 1962. *Biochemistry.* **1**:658.
29. STEIN, W. D. 1962. *Biochem. Biophys. Acta.* **59**:47.
30. STEINER, D. F., W. KEMMER, J. L. CLARK, P. E. OYER, and A. H. RUBENSTEIN. 1972. *In Handbook of Physiology. Sec. 7. Endocrinology. Vol. 1. Endocrine Pancreas.* R. O. Greep and E. B. Atwood, editors. American Physiological Society, Washington, D.C.
31. STUMPF, W. 1968. *Endocrinology* **83**:777.
32. THOMAS, P. J. 1973. *J. Endocrinol.* **57**:333.
33. WELCH, K., and K. SADLER. 1966. *Am. J. Physiol.* **210**:652.
34. WESTFALL, B. B., and E. M. LANDIS. 1936. *J. Biol. Chem.* **116**:727.